E lectronic Supplementary Material to: Contribution of Global Warming and Atmospheric Circulation to the Hottest Spring in Eastern China in 2018

Chunhui LU[1], Ying SUN[1,3], Nikolaos CHRISTIDIS[2], and Peter A. STOTT[2]

[1]*National Climate Center*, *Laboratory for Climate Studies*, *China Meteorological Administration*, *Beijing* 100081, *China*

[2]*Met Office Hadley Centre*, *Met Office*, *Exeter EX1 3PB*, *UK*

[3]*Collaborative Innovation Center on Forecast and Evaluation of Meteorological Disasters*, *Nanjing University of Information Science and Technology*, *Nanjing* 210044, *China*

ESM to : Lu, C. H., Y. Sun, N. Christidis, and P. A. Stott, 2020: Contribution of global warming and atmospheric circulation to the hottest spring in eastern China in 2018. *Adv. Atmos. Sci.*, https://doi.org/10.1007/s00376-020-0088-5. (in press)

A Brief Introduction to the Sensitivity Test Zone

Synoptic analyses indicate that the anomalous anticyclone located in the north of China blocked the high-latitude air with lower temperature from propagating to eastern China and was responsible for this extreme hot spring. Therefore, we selected the center of the anticyclone and the areas on its west side where the northwesterly airflow was prevalent as the critical area (Zone_1) to represent the role of atmospheric circulation. To test the sensitivity of the selection of the region, we also expanded the scope of the critical area to Zone_2 and Zone_3 (Fig. S1) and then partitioned the modeled spring seasons between those that correlated well with the 2018 circulation patterns over Zone_2 and Zone_3 and those with weaker correlations. The ensemble information created by this grouping is listed in Table S1. The PDF distributions of TAS with high and low correlation over Zone_1, Zone_2 and Zone_3 are shown in Fig. S4. Similar conclusions are obtained.

* The online version of this article can be found at https://doi.org/10.1007/s00376-020-0088-5.

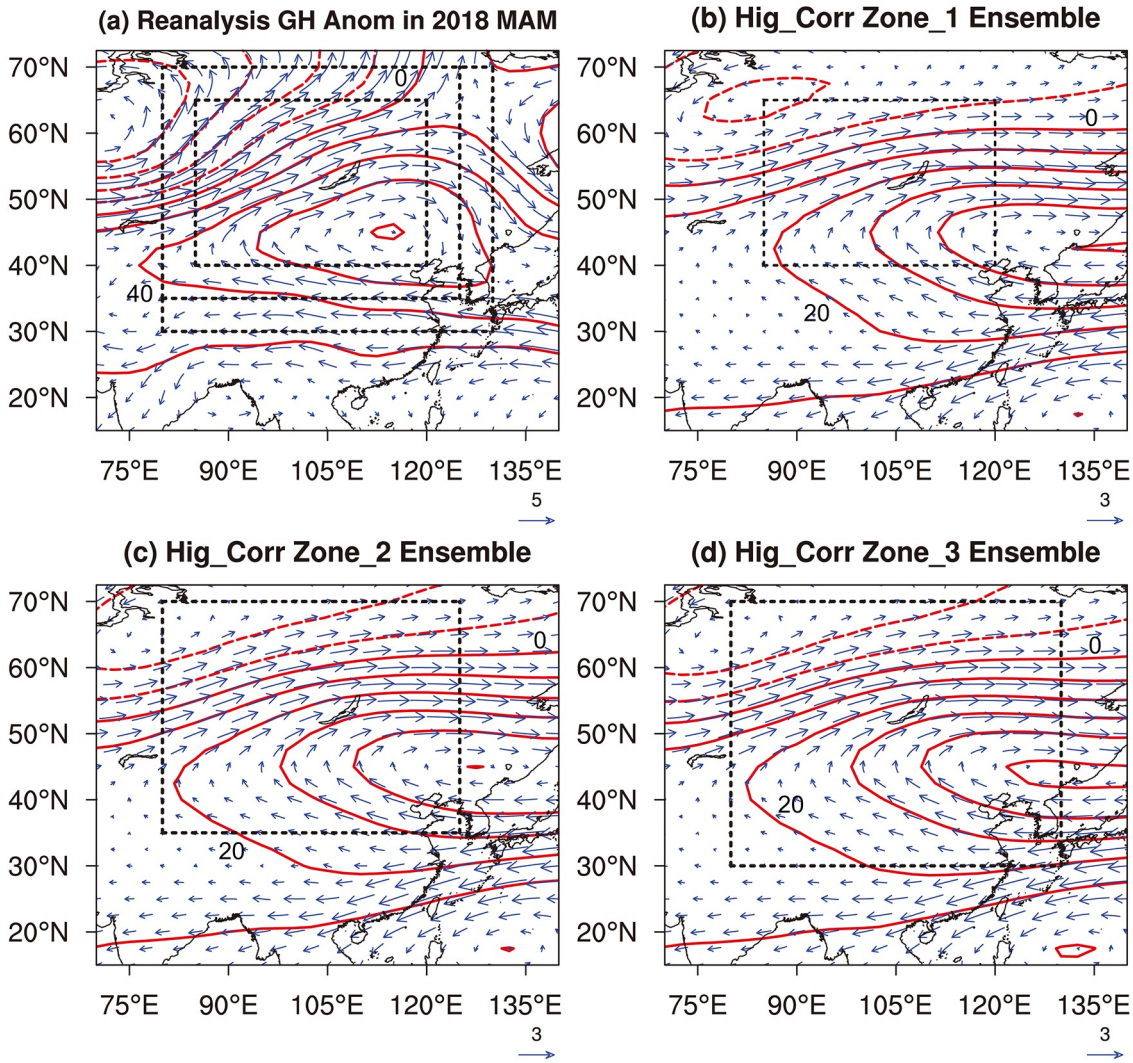

Fig. S1. (a) Geopotential height (red contours; units: gpm) and wind (blue vectors; units: m s^{-1}) spring mean anomalies (relative to 1961–1990) at 500 hPa constructed with reanalysis data for 2018. (b) As in (a) but with the mean of spring seasons extracted from the HadGEM3 extension results with the ALL experiment, for which the circulation pattern correlates well (coefficient greater than 0.6) with the 2018 reanalysis pattern over Zone_1 (40°–65°N, 85°–120° E). (c) As in (b) but for Zone_2 (35°–70° N, 80°–125° E). (d) As in (b) but for Zone_3 (30°–70° N, 80°–130° E).

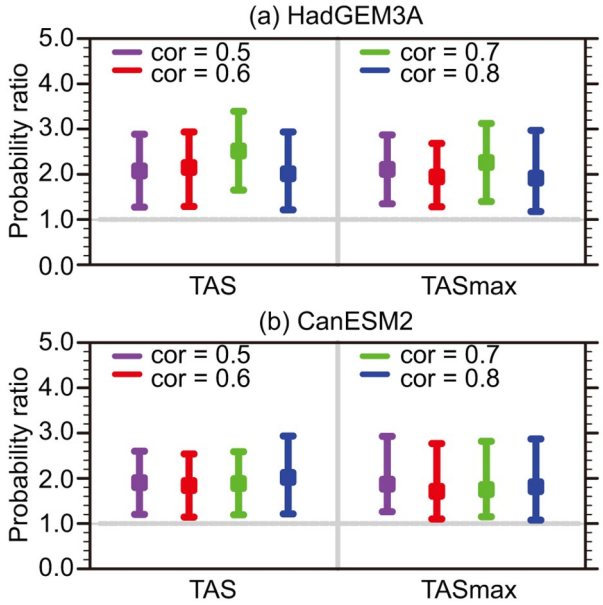

Fig. S2. Sensitivity test for the impact of the selection of the correlation coefficient threshold value. Panels (a, b) show the change in the likelihood of occurrence of extreme events when the correlation coefficient value was from 0.5 to 0.8 based on simulations from HadGEM3A and CanESM2.

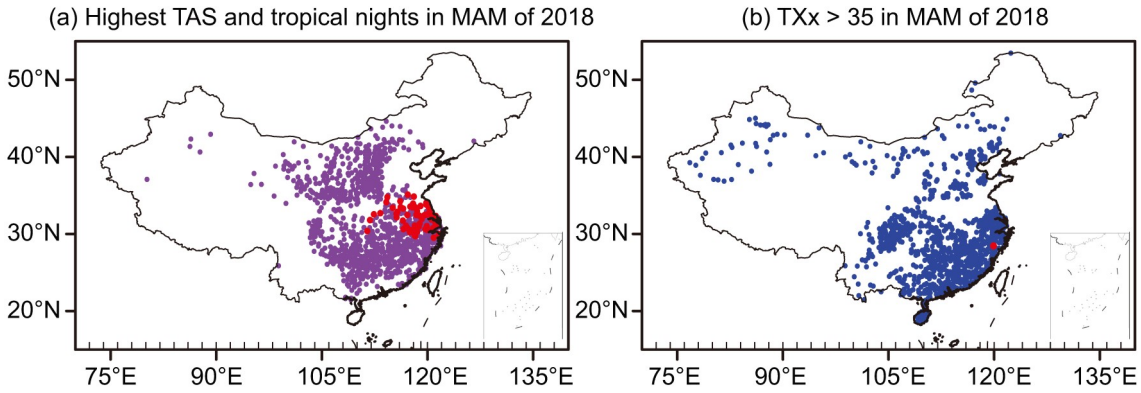

Fig. S3. (a) Stations where the spring mean TAS was recorded as its highest since 1951 (purple) and tropical nights appeared in May for the first time (red). (b) Stations where the spring maximum daily temperature was higher than 35°C. The red dot indicates the maximum value (41.7°C).

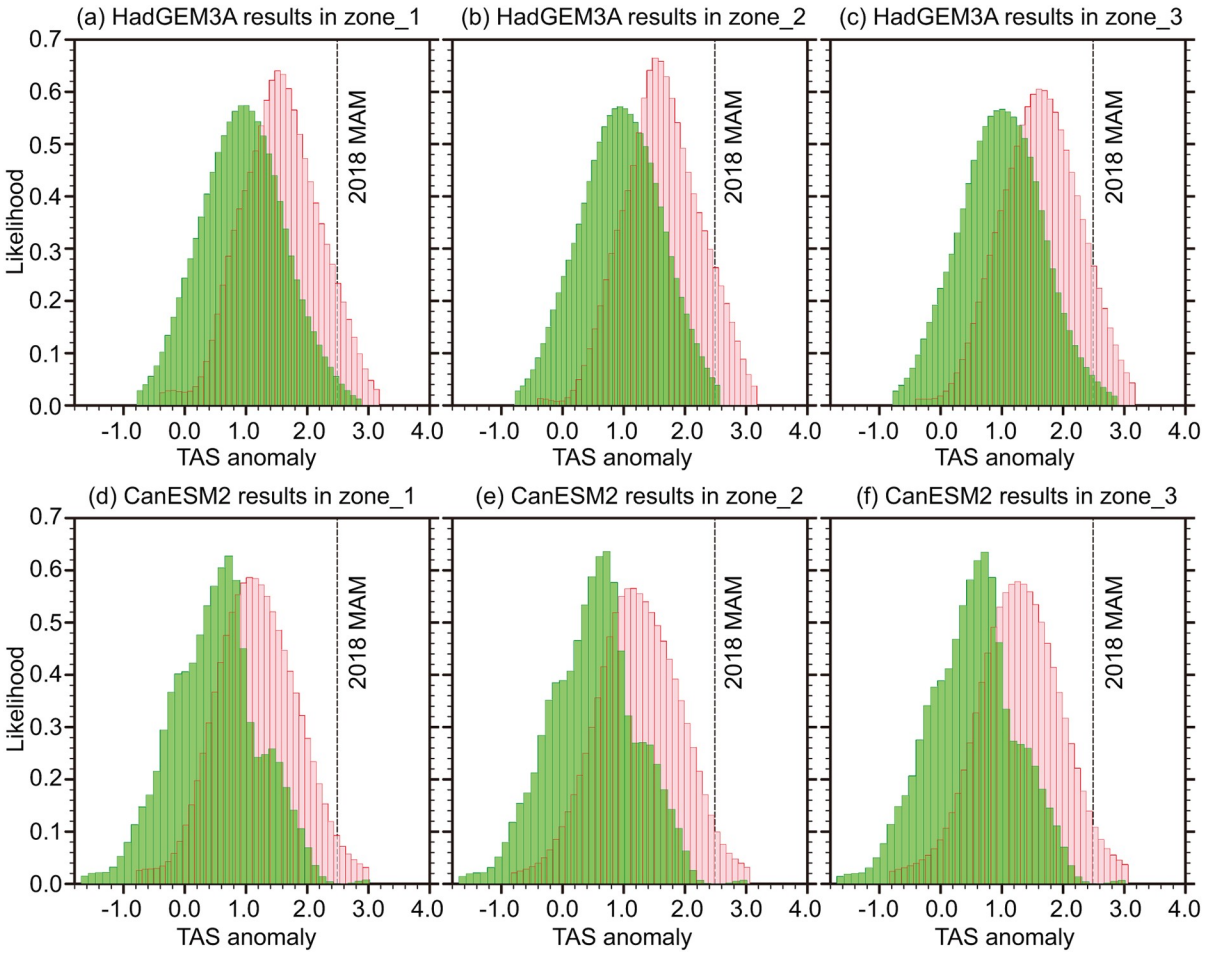

Fig. S4. Sensitivity test for the impact of the 2018 spring circulation pattern on MAM TAS anomalies. Panels (a, d) illustrate the MAM TAS anomaly distributions in the HadGEM3 extension and CanESM2 results based on simulated spring seasons with high (red) and low (green) correlations with the 2018 flow pattern over Zone_1. (b, e) As in (a, d) but for Zone_2. (c, f) As in (a, d) but for Zone_3.

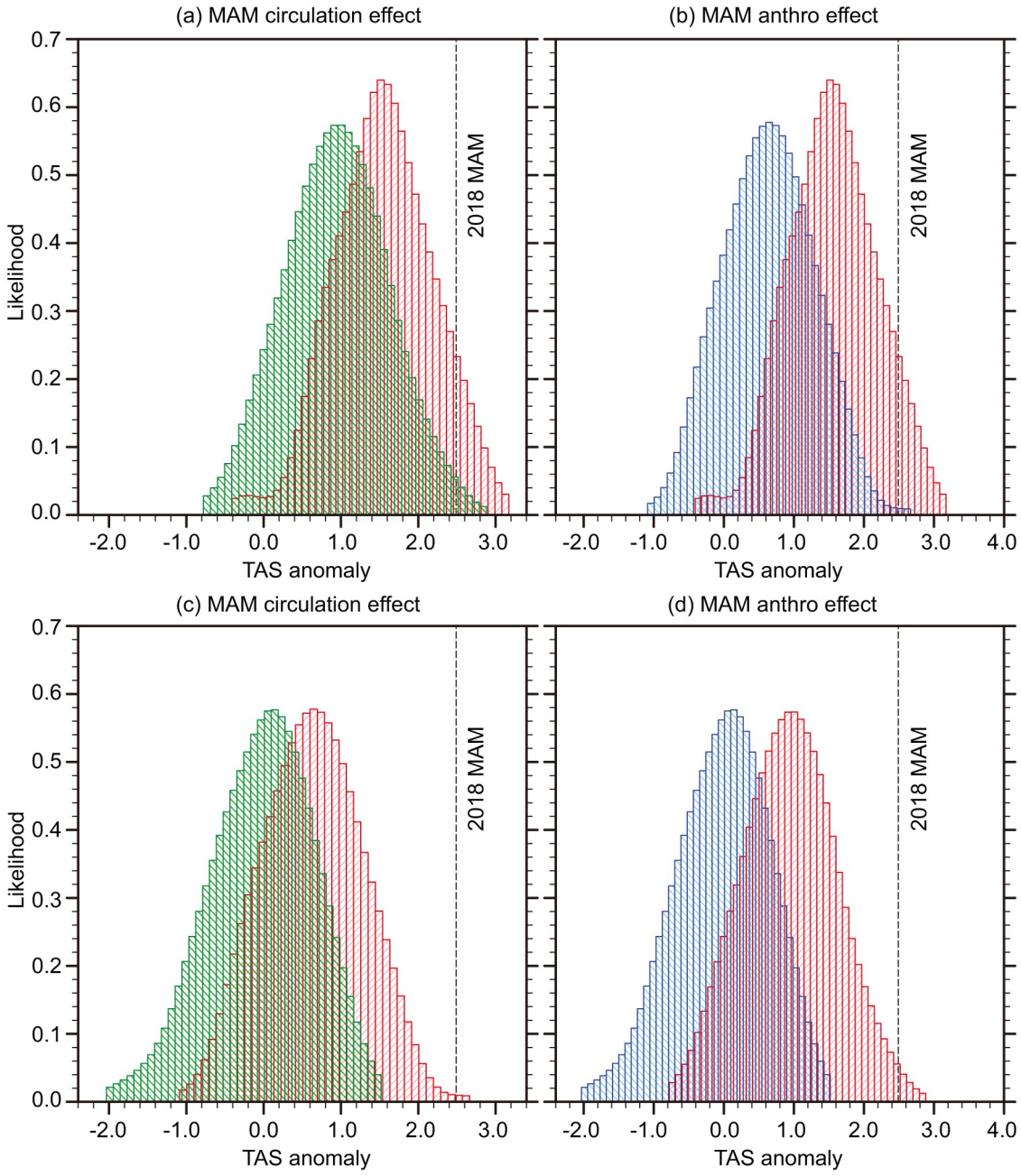

Fig. S5. Impact of the 2018 spring circulation pattern and anthropogenic forcings on MAM TAS and TASmax anomalies. Panels (a, c) illustrate the MAM TAS anomaly distributions in the HadGEM3 extension results based on simulated spring seasons with high (red) and low (green) correlations with the 2018 flow pattern under ALL forcing and NAT forcing, respectively. Panels (b, d) also illustrate the MAM TAS anomaly distributions but from model experiments with (red) and without (blue) anthropogenic forcings in high- and low-correlation ensembles, respectively.

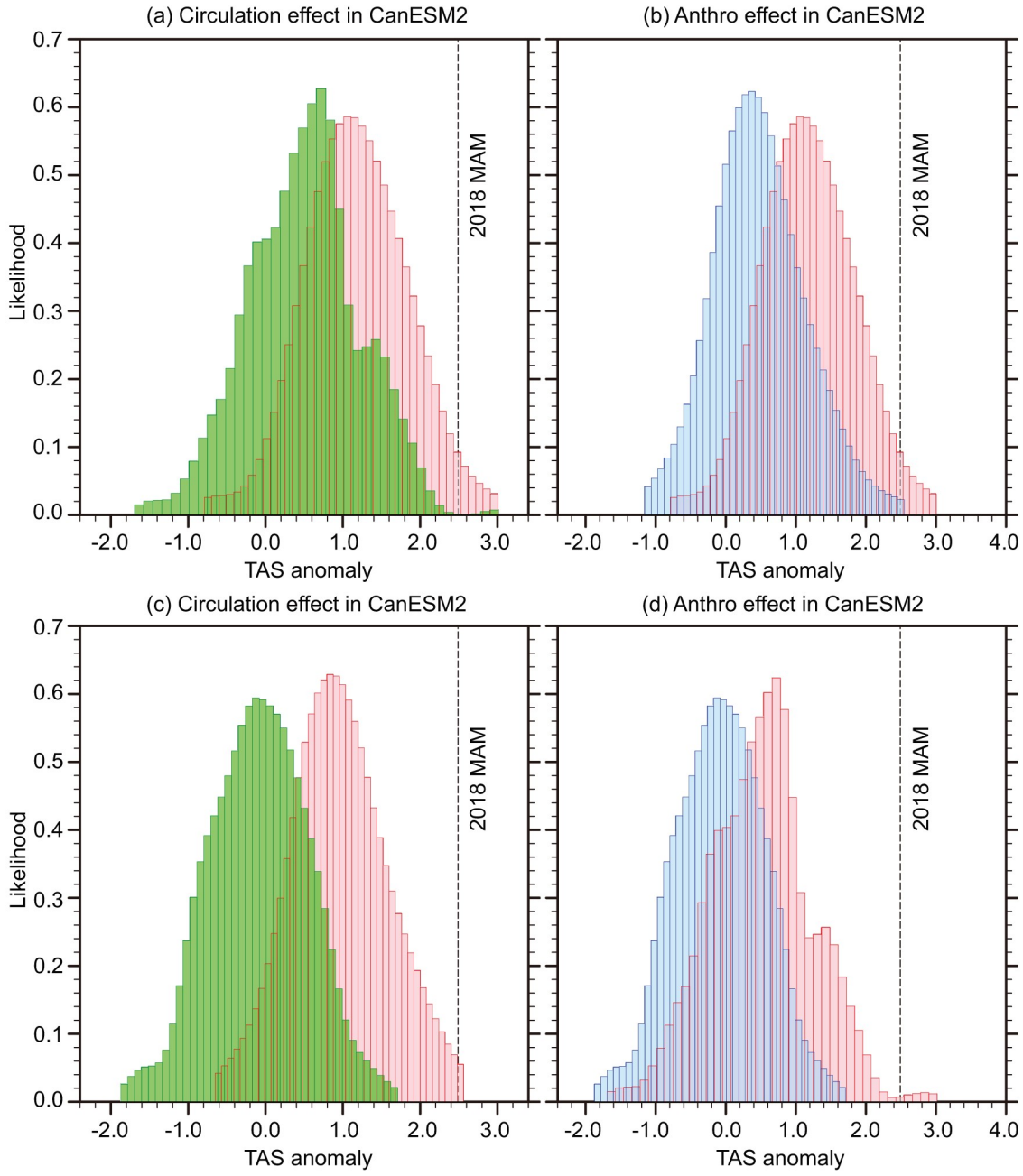

Fig. S6. As in Fig. S5 but for the CanESM2 results.

Table S1. Number of estimates of MAM TAS and TASmax from simulated spring seasons from HadGEM3A and CanESM2. The table gives the total number of spring seasons as well as the cases with high and low correlations to the 2018 circulation over Zone_1, Zone_2 and Zone_3.

		ALL			NAT		
		Total	High corr.	Low corr.	Total	High corr.	Low corr.
Zone_1	HadGEM3A	525	177	348	525	189	336
	CanESM2	500	110	390	500	118	382
Zone_2	HadGEM3A	525	155	370	525	176	349
	CanESM2	500	94	406	500	102	398
Zone_3	HadGEM3A	525	139	386	525	156	369
	CanESM2	500	81	419	500	93	407